SMAR 2017 – Fourth Conference on Smart Monitoring,
Assessment and Rehabilitation of Civil Structures

SMAR 2017

Vibration-based structural performance assessment via output-only sub-Nyquist/compressive wireless sensor data

Kyriaki Gkoktsi[1], Agathoklis Giaralis[1], Roman P. Klis[2], Vasilis Dertimanis[2], and Eleni N. Chatzi[2]

[1] City, University of London, Dept. of Civil Engineering, London, United Kingdom
[1] ETH Zürich, Department of Civil, Environmental and Geomatic Engineering, Zürich, Switzerland

ABSTRACT: This paper assesses two different approaches for efficient output-only Vibration-based Structural Health Monitoring (V-SHM) in large-scale civil engineering structures, promoting the use of dense arrays of low-power wireless sensors. Firstly, a non-uniform deterministic sub-Nyquist multi-coset sampling scheme is considered to acquire ambient stationary structural response signals. This sampling scheme is coupled with a power spectrum blind sampling technique along with the frequency domain decomposition algorithm of operational modal analysis to obtain structural modal properties. This is accomplished without necessitating either signal reconstruction in the time-domain or signal sparsity assumption. Secondly, a spectro-temporal compressive sensing approach is considered applicable to cases where signal reconstruction in time-domain is desired. The latter approach considers non-uniform in time random sampling at sub-Nyquist average rates informed by prior knowledge of signal sparsity gained through smart on-sensor operations and sensor/server communication. The usefulness and applicability of two approaches is numerically demonstrated by considering field recorded data pertaining to the monitoring of an overpass open to the traffic and of an operating on-shore wind turbine.

1 INTRODUCTION

Vibration-based structural health monitoring (V-SHM) is widely used for structural assessment, design verification, and damage detection in civil engineering structures. In most field applications, V-SHM relies on output-only linear system identification techniques to extract the dynamic properties (e.g., natural frequencies and mode shapes) of vibrating structures subject to low-amplitude operational loads (e.g., due to wind, traffic, etc.) (Brincker and Ventura (2015)). Such techniques consider acquiring and processing of *only* structural response signals recorded by relatively dense arrays of sensors. The excitation loads are not measured and are assumed to have a flat spectrum over a wide range of frequencies (i.e., white noise excitation assumption).

From a practical viewpoint, the use of wireless sensor networks (WSNs) offers low-cost and rapid V-SHM implementations compared to tethered sensors, especially in densely instrumented and geometrically complex structures (Lynch (2007)). However, the widespread adoption of WSNs in practical applications is hindered by limitations to the available wireless transmission bandwidth and by maintenance costs related to frequent sensor battery replacement (Lynch

(2007)). To this end, it has been recently recognized that WSNs operating on sub-Nyquist data acquisition schemes can provide low-power wireless sensors, while minimizing the on-sensor data storage and local processing requirements prior to wireless transmission. Such considerations reduce WSNs' upfront and maintenance costs as well as increase WSNs' reliability for quality and robust V-SHM.

In this context, advances in the field of compressive sensing (CS) have been recently considered by various researchers to facilitate cost-effective V-SHM using WSNs (O'Connor et al. (2014), Klis and Chatzi (2015; 2017), Yang and Nagarajaiah (2015), Park et al. (2014)). Specifically, CS considers *random* non-uniform in time sampling of response acceleration signal aiming to acquire a relatively small number of measurements below the Nyquist rate. The unknown full-length (Nyquist-sampled) signals are recovered, with high probability, from the acquired sub-Nyquist/compressed measurements by solving an *underdetermined* system of linear equations assuming a certain level of signal sparsity. The latter is a signal attribute related to the number of non-zero coefficients required to capture the signal energy on a given basis (see e.g. Donoho 2006), which is prerequisite in all sparse signal recovery algorithms (Vaswani and Zhan 2016). Nonetheless, the underlying signal sparsity is unknown and it is adversely affected by signal noise. To circumvent the heuristically assumed sparsity signal level in practical V-SHM settings, a spectro-temporal CS-based approach was developed by Klis and Chatzi (2015; 2017), which employs a *re-weighted Basis Pursuit De-Noising* algorithm (*rwBPDN*) (Becker et al. 2011) together with local on-sensor data processing and two-way wireless communication between sensor and server. The latter consideration allows for determining the underlying signal sparsity level prior to CS-based data acquisition, leading to improved time-domain signal recovery from the compressed measurements, at the cost of an increase wireless data transmission payload and communication protocols compared to the standard CS-based V-SHM (O'Connor et al. 2014). The recovered structural response acceleration signals can next be treated by any standard output-only V-SHM algorithm. Alternatively to the above CS-based approaches, Gkoktsi et al. (2016) adopted a *deterministic* multi-coset sub-Nyquist data acquisition scheme (Venkataramani and Bresler 2001, Tausiesakul and Gonzalez-Prelcic 2013) in conjunction with a Power Spectrum Blind Sampling (PSBS) technique (Arianandа and Leus 2012, Tausiesakul and Gonzalez-Prelcic 2013) to support V-SHM without requiring signal sparsity knowledge. The considered PSBS-based method treats response acceleration signals as *stochastic* processes (in alignment with the theory of output-only V-SHM (Brincker and Ventura 2015), aiming to retrieve the second order statistics of structural responses (i.e., covariance/power spectrum density estimates) by solving an *overdetermined* system of linear equations free from sparsity assumptions. This signal-agnostic approach is coupled with the standard frequency domain decomposition algorithm (Brincker and Ventura 2015) to estimate structural modal properties from the compressed/sub-Nyquist measurements without signal reconstruction in time. In this manner, data processing and memory requirements at both sensor and server level are minimized.

In this paper, the efficiency of the PSBS-based method (Gkoktsi et al. 2016) and of the spectro-temporal *rwBPDN* approach (Klis and Chatzi 2015 and 2017), is numerically assessed in supporting low-power WSNs that operate on sub-Nyquist data acquisition rates for output-only V-SHM. In this respect, the efficacy of the two adopted methods in extracting quality modal estimates is assessed vis-à-vis, using field recorded acceleration response data from a highway overpass under operational conditions. The performance of the two approaches is further evaluated for different data compression ratios, based on sub-Nyquist sampled data from an operating on-shore wind turbine. The remainder of the paper is organized as follows. Section 2 outlines the theoretical background of the two considered approaches. Sections 3 and 4 furnish

numerical results associated with the overpass and the wind turbine, respectively. Finally, Section 5 summarizes concluding remarks.

2 THEORETICAL BACKGROUND

2.1 Power Spectrum Blind Sampling (PSBS) approach

Let $x(t)$ be a continuous in time t real-valued wide-sense-stationary stochastic process characterized in the frequency domain by the power spectrum $P_x(\omega)$ band-limited by $2\pi/T$. It is desired to sample $x(t)$ at a rate lower than the Nyquist sampling rate $1/T$ (in Hz), while maintaining a sufficiently accurate estimate of the power spectrum $P_x(\omega)$. To this end, the multi-coset sampling strategy is herein adopted (Ariananda and Leus 2012) according to which the grid of Nyquist samples $x(nT)$ is divided into blocks of $\bar{N}$ consecutive samples and from each block only $\bar{M}$ ($<\bar{N}$) samples are selected. The resulting sampling is periodic with period $\bar{N}$; *non-uniform* since any subset of $\bar{M}$ samples may be selected from a total of $\bar{N}$ Nyquist-rate samples within each block; and deterministic since the position of the $\bar{M}$ samples on the Nyquist grid of samples $x(nT)$ is defined *a priori* and applies to all considered blocks. The above sampling strategy can be implemented by utilizing $\bar{M}$ interleaved ADC units operating at a sampling rate of $1/(\bar{N}T)$. At the *m-th* (m= 0, 1, …, $\bar{M}$-1) unit, the discrete-time signal $x[n]= x(n/T)$ is first shifted by n_m samples and then uniformly sampled at $1/\bar{N}T$ (in Hz). In this respect, an average sampling rate of $\bar{M}/(\bar{N}T)$ (in Hz) is defined, which is associated with the compression ratio $\bar{M}/\bar{N}$, with $0 \leq \bar{M}/\bar{N} \leq 1$, corresponding to lower values at stronger signal compression. Notably, the limiting case of $\bar{M}=\bar{N}$ (i.e., $\bar{M}/\bar{N}=1$) pertains to the Nyquist rate. Finally, the shifting values n_m are collected in the sequence $\mathbf{n}=[n_0, n_1,\ldots, n_{\bar{M}-1}]$ which defines the multi-coset sampling pattern.

Consider, next, an array of D sensors and $\bar{M}$ cosets. The cross-correlation function of the acquired measurements $y_{m_i}^{d_a}[l]$, $y_{m_j}^{d_b}[l]$ can be computed for all m_i, m_j = 0,1,…, $\bar{M}$-1 cosets and d_a, d_b=1, 2,…, D sensors as in $r_{y_i^a,y_j^b}[k] = \mathrm{E}_y\left\{y_{m_i}^{d_a}[l]\, y_{m_j}^{d_b}[l-k]\right\}$, where $\mathrm{E_a}\{\cdot\}$ is the mathematical expectation operator with respect to a. Further, the following relation holds (Gkoktsi et al. 2016)

$$\mathbf{r}_{y^a y^b} = \mathbf{R}_c \mathbf{r}_{x^a x^b}\,, \tag{1}$$

where $\mathbf{r}_{y^a y^b} \in \mathbb{R}^{\bar{M}^2(2L+1)\times D}$ is a matrix collecting the output cross-correlation sequences $r_{y_i^a,y_j^b}[k]$ computed within the range (support) $-L \leq k \leq L$. Similarly, $\mathbf{r}_{x^a x^b} \in \mathbb{R}^{\bar{N}(2L+1)\times D}$ is a matrix collecting the input cross-correlation sequences of the traditionally sampled signals (at Nyquist rate or above), given in $r_{x^a x^b}[k] = \mathrm{E}_x\left\{x^{d_a}[n]\, x^{d_b}[n-k]\right\}$, and computed for all d_a and d_b sensors in the above range. Further, $\mathbf{R}_c \in \mathbb{R}^{\bar{M}^2(2L+1)\times\bar{N}(2L+1)}$ is a sparse pattern correlation matrix populated with the pattern cross-correlations (Ariananda and Leus 2012) $r_{c_i,c_j}[n] = \delta[n-(n_{m_i}-n_{m_j})]$, where $\delta[n]$=1 for n=0 and $\delta[n]$=0 for $n\neq 0$. Note that Eq. (1) defines an overdetermined system of linear equations which can be solved for $\mathbf{r}_{y^a y^b}$ without any sparsity assumptions, provided that $\mathbf{R}_c$ is full column rank. The latter is satisfied for $\bar{M}^2 \geq \bar{N}$ (Tausiesakul and Gonzalez-Prelcic 2013, Ariananda and Leus 2012). An unbiased estimator of the output cross-correlation sequence $r_{y_i^a,y_j^b}[k]$ is then adopted (Gkoktsi et al. 2016) and used together with the DFT matrix, $\mathbf{F}_{(2L+1)\bar{N}} \in \mathbb{C}^{\bar{N}(2L+1)\times\bar{N}(2L+1)}$ to obtain an estimate of the input cross-spectra $\mathbf{s}_{x^a x^b}$ at the discrete frequencies ω=[0, $2\pi/(2L+1)\,\bar{N}$, … , $2\pi((2L+1)\,\bar{N}$ -1)/$(2L+1)\,\bar{N}$] (Tausiesakul and Gonzalez-Prelcic 2013)

$$\hat{\mathbf{s}}_{x^a x^b} = \mathbf{F}_{(2L+1)\bar{N}}\left(\mathbf{R}_c^{\mathrm{T}}\tilde{\mathbf{W}}^{-1}\mathbf{R}_c\right)^{-1}\mathbf{R}_c^{\mathrm{T}}\tilde{\mathbf{W}}^{-1}\hat{\mathbf{r}}_{y^a y^b}\,. \tag{2}$$

In the above equation, $\tilde{\mathbf{W}}$ is a weighting matrix, the symbol "^" denotes matrix estimation, and the superscript "−1" denotes matrix inversion. The solution of Eq. (2) relies on the weighted least square criterion $\hat{\mathbf{r}}_{x^a x^b} = \arg\min_{\mathbf{r}_{x^a x^b}} \| \hat{\mathbf{r}}_{y^a y^b} - \mathbf{R}_c \mathbf{r}_{x^a x^b} \|^2_{\tilde{\mathbf{W}}}$, where $\| \mathrm{a} \|^2_{\tilde{\mathbf{W}}} = \mathrm{a}^{\mathrm{T}} \tilde{\mathbf{W}} \mathrm{a}$ is the weighted version of the Euclidean norm.

2.2 Spectro-Temporal Compressive Sensing via rwBPDN

Spectro-Temporal Compressive Sensing (*STCS*) is based on the formulation of the missing data problem investigated by a number of authors (Candes 2007 and 2011, Becker 2011). Let $\mathbf{x}_i = [x_{1i}, x_{2i}, ..., x_{Ni}]^{\mathrm{T}} \in \mathbb{R}^N$ designate the complete i^{th} signal recorded by the i^{th} sensor of N data samples. The missing data estimation problem can be expressed as:

$$\mathbf{y}_i = \mathbf{S}\mathbf{x}_i \,. \tag{3}$$

The problem may be formulated as the task of inferring the full response time-series $\mathbf{x}_i \in \mathbb{R}^N$ given the incomplete observation vector $\mathbf{y}_i \in \mathbb{R}^M$ ($M \ll N$), and the selection matrix $\mathbf{S} \in \mathbb{C}^{M \times N}$, so that (3) holds. A spectral representation of the complete response signal $\mathbf{x}_i$ is accomplished using the orthonormal basis $\mathbf{A} \in \mathbb{C}^{N \times N}$ of the Discrete Fourier Transform (DFT) as:

$$\mathbf{x}_i = \mathbf{A}\mathbf{c}_i, \text{ where } \quad \mathbf{A}_{i,l} = \frac{1}{\sqrt{N}} e^{-j2\pi i \frac{l}{N}}, \tag{4}$$

where $\mathbf{c}_i = [c_{1i}, c_{2i}, ..., c_{Ni}]^{\mathrm{T}} \in \mathbb{R}^N$ is a sparse vector of coefficients. From the above equations, the observed vector $\mathbf{y}_i$ can be cast in the form

$$\mathbf{y}_i = \mathbf{S}\mathbf{A}\mathbf{c}_i \,. \tag{5}$$

As demonstrated in previous work of the authors (Klis and Chatzi 2015 and 2017) the former representations allow to reconstruct the original (i.e., complete) response signal $\mathbf{x}_i$, by solving (5) for $\mathbf{c}_i$ and applying the transformation in (4). The sought solution for $\mathbf{c}_i$ may be obtained via the following optimization problem, known as the *reweighed Basis Pursuit De-Noising problem (rwBPDN)* (Becker 2011)

$$\hat{\mathbf{c}}_i = \arg\min_{\mathbf{c}_i} \| \mathbf{W}\mathbf{c}_i \|_1 \text{ subject to } \| \mathbf{y}_i - \mathbf{S}\mathbf{A}\mathbf{c}_i \|_2 \le \epsilon \,, \tag{6}$$

where $\mathbf{W} = diag([w_1, w_2, ..., w_N])$, indicating the salient spectral elements. These weighting coefficients are the key feature of the Spectro-Temporal Compressive Sensing formulation. The weighting matrix $\mathbf{W}$ is defined upon selection of a suitable threshold ϵ_l, which defines the elements to be included in the so-called support vector **U.** The support components are defined locally at the node level, and eventually transmitted to the server, where the weighting matrix is formed and the level of sparsity is decided upon. Sparsity *k* is defined as the ratio of the number of harmonic components, *K*, in the signal over its full dimension, *N*. The original signal is then reconstructed using the coefficient vector $\hat{\mathbf{c}}_i$ defined in equation (6), via projection back to the time domain as in

$$\hat{\mathbf{x}}_i = \mathbf{A}\hat{\mathbf{c}}_i \,. \tag{7}$$

For further details on the steps involved, as well as the exchange of operations between the server and the nodes, the interested reader is referred to the work of Klis and Chatzi (2015, 2017).

3 ASSESSMENT FOR OPERATIONAL MODAL ANALYSIS

The effectiveness of the PSBS-based approach for structural modal properties extraction is herein numerically assessed vis-à-vis the spectro-temporal *rwPBDN* method by considering response acceleration signals recorded in the Bärenbohlstrasse overpass in Zürich, Switzerland (Klis *et al* 2016). Specifically, a dataset of D=18 vertical bridge acceleration responses of 107460 samples each is considered, acquired under operational conditions at a uniform sampling rate of 200Hz. The raw data are first pre-processed (baseline adjustment and 4th-order Butterworth band-pass filtering within the frequency range of [0.15, 50] in Hz) to remove the mean value and any potential low-frequency trend within each acceleration response. The PSBS-based approach is applied assuming compression ratios (*CRs*) at 31% ($\bar{M}$=5, $\bar{N}$=16, $\mathbf{n}$ = [0, 1, 2, 5, 8]^{T}), and at 11% ($\bar{M}$=14, $\bar{N}$=128, $\mathbf{n}$= [0, 1, 2, 6, 8, 20, 29, 38, 47, 50, 53, 60, 63, 64]^{T}) below the Nyquist frequency to retrieve the sub-Nyquist sampled measurements $y_m^d[l]$ (d=1,2,…,18, m=1,2,…,M). The latter are next collectively considered to obtain the output cross-correlation sequences, $\hat{r}_{y_i^a,y_j^b}[k]$, which are further used in Eq. (2) to estimate the power spectral density (PSD) response matrix, $\hat{\mathbf{s}}_{x^a x^b}$, from the 18 devices. The *PSD* matrix is subsequently fused within the standard FDD algorithm (Brincker and Ventura 2015) to extract the modal properties of the monitored bridge, which are reported in Table 1 for the first four modes of vibration.

Table 1. Bridge modal estimates obtained from a conventional approach applied to the full-length dataset (*CR*=100%), the PSBS-based FDD *CR*={31%,11%}, and the rwPBDN NeXT-ERA at *CR*={36%,11%}

	Conventional	*PSBS*				*rwPBDN*			
	CR=100%	*CR*=31%		*CR*=11%		*CR*=36%		*CR*=11%	
Mode	*F* [Hz]	d*F*/*F* [%]	*MAC*	d*F*/*F* [%]	*MAC*	d*F*/*F* [%]	*MAC*	d*F*/*F* [%]	*MAC*
1	7.617	0.37	1.000	1.02	0.997	0.63	0.997	0.52	0.983
2	10.352	0.44	0.998	0.31	0.987	0.18	0.981	0.32	0.976
3	11.719	0.84	1.000	0.46	0.998	0.19	0.992	0.14	0.990
4	12.598	0.47	0.972	0.50	0.960	1.22	0.960	0.78	0.943

The *STCS-rwPBDN* approach is further applied to a dataset of 18 two-minute long measurements $\mathbf{x}_i \in \mathbb{R}^{N\times 1}, (i=1\ldots 18, N=11776)$, down-sampled at 100 Hz. The considered dataset is first partitioned into R= 29 windows (frames) of N_R= 400 samples, and each window is projected into the spectral domain (see also left panel in Figure 1). Following the methodology in Section 2.2, the spectral coefficients per data frame are then thresholded with a value $\epsilon_{ij} = \epsilon_l \| \mathbf{c}_{ij} \|_1 / N_R$, $j=1\ldots R$, which pertains to $\epsilon_l = 1.5$ in this case study, yielding the spectral domain elements illustrated in the left panel of Figure 1. The selected support elements are further used to form a weighting matrix $\mathbf{W}_{ij}$ per data frame. Considering next two different *CRs* at {36%,11%}, the compressed samples $\mathbf{y}_i$ (denoted with a cross in Figure 1) are selected and used to retrieve the reconstructed time-domain sequence plotted in Figure 1 by a broken line. The Natural eXcitation Technique (NeXT) combined with the Eigensystem Realization Algorithm (ERA) are then used to extract the bridge modal propertied presented in Table 1. This table also reports the modal estimates obtained from a conventional approach applied to the full-length dataset (i.e. *CR*=100%), hereafter referred to as the "exact solution". In this respect, the percentage difference error, d*F*/*F*, and the Modal Assurance Criterion (MAC) (Brincker and Ventura (2015)) are used to quantify the accuracy of the modal estimates extracted from the two alternative sub-Nyquist approaches with respect to the exact solution. From Table 1, it is readily observed that the two alternative approaches perform equally well in extracting quality modal estimates even from the processing of 89% fewer measurements compared to conventional approaches (i.e., at

CR=11%), yielding natural frequencies with small errors (below 1.3%), and mode shapes of high MAC values (close to unity) in all cases considered.

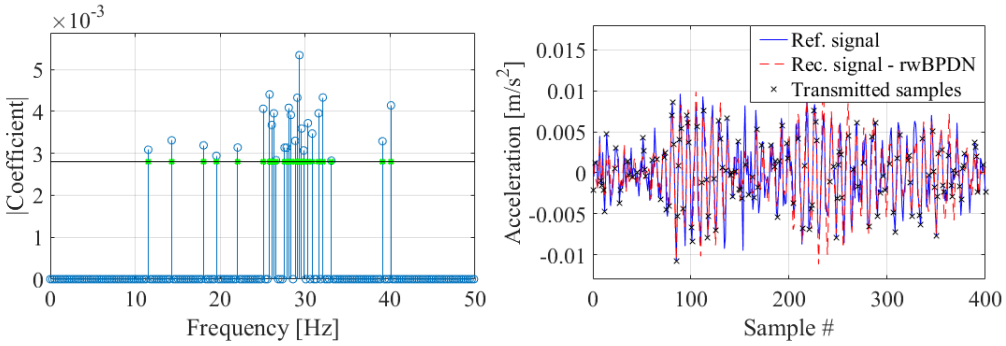

Figure 1. Spectral domain projection (left) and time-domain recovery (right) of data-frame #4, channel #1 at CR=36%. Crosses indicate transmitted samples used in the recovery process.

4 ASSESSMENT FOR SIGNAL RECOVERY IN TIME AND IN FREQUENCY DOMAIN

Arguably, the accuracy of the two considered approaches strongly depends on the efficiency of the associated recovery operation (i.e., power spectral recovery in the PSBS-based approach, and time-domain signal reconstruction in the *STCS-rwPBDN* method) applied on the acquired compressed measurements. For both approaches, the pertinent recovery performance is numerically assessed herein as a function of the signal compression level achieved by the adopted sub-Nyquist sampling schemes, using field-recorded acceleration responses from an operational Wind Turbine (WT) in Lübbenau, Germany (Klis and Chatzi 2015). The recorded WT data were conventionally acquired at a uniform sampling rate of 200 Hz.

4.1 PSBS approach for frequency domain signal recovery

For the numerical evaluation of the power spectral recovery in the *PSBS*-based approach (sub-section 2.1), a WT pre-processed (i.e., baseline adjusted and filtered) acceleration time-series is employed herein, in which the stationarity hypothesis is confirmed at the 95% confidence level. The accuracy of the recovered *PSD* estimate in Eq. (2) is assessed at two different *CRs* of approximately 11% (for $\bar{M}$=14, $\bar{N}$=128, and $\mathbf{n}$= [0,1,2,6,8,20,29,38,47,50,53,60,63,64]^T), and 31% (for $\bar{M}$=5, $\bar{N}$=16, and $\mathbf{n}$= [0,1,2,5,8]^T), which pertain to 89% and 69% fewer data compared to the uniformly-sampled full-length signal. For the two adopted *CRs*, the obtained *PSD* estimates are presented in Figure 2 (solid gray curve), and plotted against the standard Welch periodogram (broken black curve), which is computed for the full-length signal of 172420 samples, assuming 4096 (=2^{12}) FFT points, eight overlapping segments with 50% overlap, windowed with a Hanning function (Marple 1987). Notably, the *PSD* curves in Figure 2 are normalized to their maximum amplitude to facilitate comparison. For *CR*=11%, the left panel of Figure 2 shows that the recovered *PSD* curve can closely approximate the Welch periodogram in the frequency range below 5 Hz, where the important WT modal information lies. However, the retrieved *PSD* estimate deviates significantly from the Welch periodogram at higher frequencies (i.e., above 5 Hz), and especially in the anti-resonance ranges. These discrepancies are considerably reduced at the higher *CRs* and the *PSD* recovery from an increased number of measurements, as clearly indicated in right panel of Figure 2 for the *PSBS*-based approach operating at *CR*=31%.

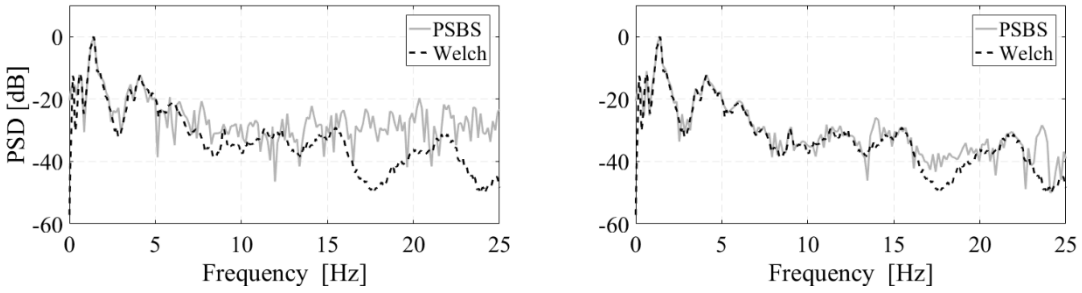

Figure 2. PSD estimates: Wlech periodogram at Nyquist rate compared with PSBS approach for *CR*=11% (left), and *CR*=31% (right)

4.2 STCS-rwBPDN approach for time domain signal recovery

The reconstruction performance of the *STCS-rwBPDN* framework is next assessed for two compression ratios at *CR* = {30%, 45%}. For a given WT acceleration response, the underlying signal support **U** is first computed to define the signal's sparsity level, *k* (i.e., number of components in the spectral domain), as well as the variance of the noisy component, i.e., the complementary set of the support (remaining part of the spectral representation). As elaborated upon in the work of Klis and Chatzi (2015; 2017), this is used to prescribe error bounds on the reconstructed signal. For the two considered *CRs*, the obtained signal reconstruction estimates are illustrated in Figure 3 for an acceleration time-window of 400 samples. Comparing the two panels in Figure 3, it becomes evident that the increase in the number of transmitted samples results in narrowing the estimated maximal error bounds. Figure 3 also demonstrates the potential of the proposed framework, when applied in windows of non-stationary response signals, albeit necessitating higher compression rates than the conventional stationary case. The delivered error bounds allow for attributing some level of confidence on the undertaken signal reconstruction operation, which offers a benefit over the alternative (plain) *BPDN* approach adopted by O'Connor et al. (2014).

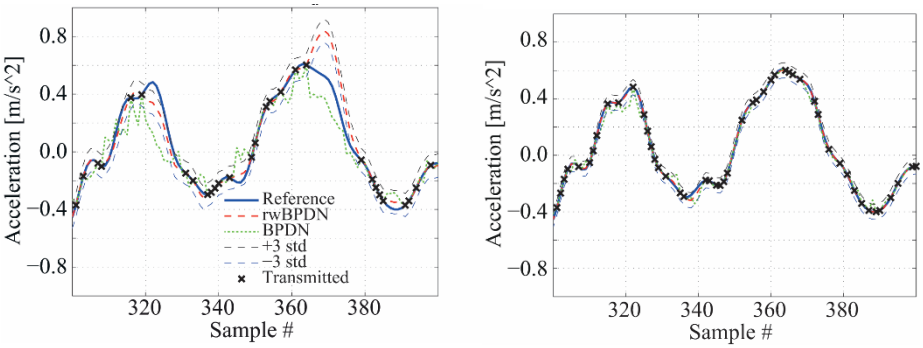

Figure 3. Effect of the increase of transmission level *CR* on the estimated error bounds: *CR*=30% (left), *CR*=45% (right). Figure reused from (Klis and Chatzi (2015)).

5 CONCLUDING REMARKS

The performance of a PSBS-based method and a spectro-temporal *rwBPDN*-based approach has been numerically assessed in undertaking output-only V-SHM using WSNs. Both the approaches aim to reduce the wireless data transmission payloads by considering compressed structural acceleration responses acquired at sub-Nyquist rates. The PSBS method recovers power spectral estimates directly in the compressed domain while the *STCS-rwBPDN* approach provides

reconstructed signals in time-domain. The validation of the two approaches is carried out on field-recorded data obtained from an overpass, and from an operating wind turbine. It is shown that both considered approaches can accurately identify the underlying structural modal properties for compression ratios (*CRs*)as low as 11%, yielding modal estimates of similar accuracy. It is further shown that the efficacy of the two approaches relies on the pertinent recovery operations applied on compressed data, which are significantly affected by the adopted *CR*.

6 REFERENCES

Arianandа, D.D., and Leus, G., 2012, Compressive Wideband Power Spectrum Estimation. *Signal Process IEEE Trans*, 60(9): 4775–4789.

Becker, S., Bobin, J., and Cands, E.J., 2011, Nesta: A fast and accurate first-order method for sparse recovery. *SIAM Journal on Imaging Sciences*, 4(1): 1–39.

Brincker, R, and Ventura, CE. 2015. *Introduction to Operational Modal Analysis*. Chichester, UK: John Wiley & Sons, Inc.

Candés, E. and Plan, Y., 2011, A probabilistic and ripless theory of compressed sensing. *Information Theory, IEEE Transactions on*, 57(11):7235-7254.

Candés, E. and Romberg, J., 2007, Sparsity and incoherence in compressive sampling. *Inverse Problems*, 23(3):969.

Donoho, D.L., 2006, Compressed sensing. *IEEE Trans Inf Theory*, 52(4): 1289–1306.

Gkoktsi, K., Giaralis, A., and TauSiesakul, B., 2016, Sub-Nyquist signal-reconstruction-free operational modal analysis and damage detection in the presence of noise. *In: Lynch JP (ed) SPIE Smart Structures and Materials + Nondestructive Evaluation and Health Monitoring*, Las Vegas, NV.

Klis, R., and Chatzi, E., 2015, Data recovery via Hybrid Sensor Networks for Vibration Monitoring of Civil Structures. *Int J Sustain Mater Struct Syst*, 2(1/2): 161-184.

Klis, R., and Chatzi, E.N., 2017, Vibration Monitoring via Spectro-Temporal Compressive Sensing for Wireless Sensor Networks. *Structure and Infrastructure Engineering*, 13(1): 195–209.

Klis, R., Chatzi, E., and Spiridonakos, M., 2016, Validation of Vibration Monitoring via Spectro-Temporal Compressive Sensing for Wireless Sensors Networks using bridge deployment data, *Proceedings of the 8th International Conference on. Bridge Maintenance, Safety and Management (IABMAS 2016), June 26 - 30*.

Lynch, J.P., 2007, An overview of wireless structural health monitoring for civil structures. *Phil. Trans. R. Soc. A*, 365(1851): 345-372.

Marple, S.L., 1987. *Digital Spectral Analysis with Applications*. Englewood Cliffs, New Jersey: PTR Prentice Hall.

O'Connor, S.M., Lynch, J.P., and Gilbert, A.C., 2014, Compressed sensing embedded in an operational wireless sensor network to achieve energy efficiency in long-term monitoring applications. *Smart Mater Struct*, 23(8): 085014.

Park, J.Y., Wakin, M.B., and Gilbert A.C., 2014, Modal analysis with compressive measurements. *IEEE Trans Signal Process*, 62(7): 1655–1670.

Tausiesakul, B., and Gonzalez-Prelcic, N., 2013, Power Spectrum Blind Sampling Using Minimum Mean Square Error and Weighted Least Squares. *In: 47th Asilomar Conference Signals, Systems and Computers (ACSSC)*, 153–157.

Vaswani, N., and Zhan, J., 2016, Recursive Recovery of Sparse Signal Sequences from Compressive Measurements: A Review. *IEEE Trans Signal Process*, 64(13): 3523–3354.

Venkataramani, R., and Bresler, Y., 2001, Optimal sub-nyquist nonuniform sampling and reconstruction for multiband signals. *IEEE Trans Signal Process*, 49(10): 2301–2313.

Yang, Y., and Nagarajaiah, S., 2015, Output-only modal identification by compressed sensing: Non-uniform low-rate random sampling. *Mech Syst Signal Process*, 56–57: 15–34.